Resolving the controversies about the 'nearly cubic' and other phases of $Sr_{1-x}Ca_xTiO_3$ ($0 \leq x \leq 1$): II. Comparison of phase transition behaviours for $x = 0.40$ and 0.43

2006 J. Phys.: Condens. Matter 18 1899

(http://iopscience.iop.org/0953-8984/18/6/007)

INSTITUTE OF PHYSICS PUBLISHING JOURNAL OF PHYSICS: CONDENSED MATTER

J. Phys.: Condens. Matter **18** (2006) 1899–1912 doi:10.1088/0953-8984/18/6/007

Resolving the controversies about the 'nearly cubic' and other phases of $Sr_{1-x}Ca_xTiO_3$ ($0 \leqslant x \leqslant 1$): II. Comparison of phase transition behaviours for $x = 0.40$ and 0.43

Sanjay Kumar Mishra[1], Rajeev Ranjan[1], Dhananjai Pandey[1], Pierre Ranson[2], Robert Ouillon[2], Jean-Paul Pinan-Lucarre[2] and Philippe Pruzan[2,3]

[1] School of Materials Science and Technology, Institute of Technology, Banaras Hindu University, Varanasi-221005, India
[2] Laboratoire de Physique des Milieux Condensés, UMR 7602, Université Pierre et Marie Curie, 140 rue de Lourmel, 75015 PARIS, France

Received 30 June 2005, in final form 2 November 2005
Published 24 January 2006
Online at stacks.iop.org/JPhysCM/18/1899

Abstract

The phase transition behaviour of two 'nearly cubic' compositions, $x = 0.40$ and 0.43, of $Sr_{1-x}Ca_xTiO_3$, representative of *Pbnm* and *Pbcm* space group structures, has been investigated using temperature dependent dielectric, x-ray diffraction and Raman scattering techniques. For $x = 0.40$, a first order antiferroelectric phase transition occurs around 364 K followed by an antiferrodistortive phase transition involving the R point ($q = \frac{1}{2}\ \frac{1}{2}\ \frac{1}{2}$) instability at ~800 K. For $x = 0.43$, on the other hand, there is no antiferroelectric phase transition. Instead, two antiferrodistortive transitions around 463 and 850 K linked with the M ($q = \frac{1}{2}\ \frac{1}{2}\ 0$) and R ($q = \frac{1}{2}\ \frac{1}{2}\ \frac{1}{2}$) point instabilities, respectively, are observed. Both the compositions also exhibit qualitatively different types of phase transitions below room temperature. Evidence for a new phase transition at low temperatures is presented for $x = 0.43$.

1. Introduction

In the preceding paper (henceforth referred to as Part I), we discussed the evolution of the structure of $Sr_{1-x}Ca_xTiO_3$ (SCT) as a function of Ca^{2+} content at room temperature. It was shown that in the composition range $0.35 < x < 0.70$, the elementary perovskite cell parameters are very close to each other and the powder x-ray diffraction patterns appear like that of a 'nearly cubic' phase. It was also shown that the 'nearly cubic' phase region of SCT can be divided into two composition domains, $0.35 < x \leqslant 0.40$ and $0.40 < x < 0.70$, corresponding to two different structures with space groups *Pbcm* and *Pbnm*, respectively.

[3] Deceased.

In the present paper, we compare phase transition behaviours of two 'nearly cubic' SCT compositions, namely $x = 0.40$ (SCT40) and $x = 0.43$ (SCT43), representative of the $Pbcm$ and $Pbnm$ space groups, respectively, using dielectric, x-ray diffraction and Raman scattering measurements. It is shown that for $x = 0.40$ a first order antiferroelectric (AFE) phase transition occurs around 364 K, which is followed by an antiferrodistortive phase transition involving the R point ($q = \frac{1}{2}\ \frac{1}{2}\ \frac{1}{2}$) instability at ~800 K. For $x = 0.43$, on the other hand, the AFE phase transition is not present. This composition exhibits two antiferrodistortive phase transitions around 463 and 850 K corresponding to the M ($q = \frac{1}{2}\ \frac{1}{2}\ 0$) and R ($q = \frac{1}{2}\ \frac{1}{2}\ \frac{1}{2}$) point instabilities, respectively. The phase transitions occurring below room temperature are also shown to be quite different for the two compositions.

2. Experimental details

The details of SCT sample preparation are given in part I. Dielectric measurements were carried out on 98% dense pellets of 0.1 cm thickness and 1.3 cm diameter. For dielectric measurements, both the faces of sintered circular pellets were gently polished with 0.25 μm diamond paste and then washed with acetone to clean off the surfaces. Isopropyl alcohol was then applied to remove the moisture, if any, left on the pellet surface. Fired-on silver paste applied on both the faces of the pellets was first dried at 373 K and then cured by firing at 773 K for 5 min. Temperature was measured with an accuracy of 1 K by a Keithley thermometer (model 740) using a chromel–alumel thermocouple. A Hewlett Packard 4192 impedance analyser was used for the measurement of capacitance and loss tangent ($\tan\delta$).

The low temperature x-ray diffraction data were collected using a 18 kW rotating Cu anode based Rigaku powder diffractometer (RINT 2000/PC series) operating in the Bragg–Brentano geometry and fitted with a He closed cycle low temperature attachment (12–300 K). The high temperature x-ray diffraction studies above 300 K were carried out on a 12 kW rotating Cu anode based Rigaku powder diffractometer (model D/max-A) fitted with a Rigaku high temperature attachment. A curved crystal monochromator in the diffraction beam was used for both the low and high temperature XRD measurements. The sample temperature was stable within ± 1 K during these measurements. All the XRD data were collected at a scan speed of 1° min^{-1} at a step ($\Delta 2\theta$) of 0.02°. The Rietveld refinements were carried out in the manner outlined in part I.

The Raman scattering measurements at high temperatures were carried out with a Jobin Yvon RAMANOR HG-2S Raman spectrometer in oblique geometry. The polished pellets with good reflectivity were inserted into a larger copper block located in a temperature controlled furnace. The experiments were performed between room temperature and 473 K. The temperature was stable within ± 0.5 K during these measurements. For the low temperature measurements, the samples were mounted in an optical He cryostat from SMC Instruments. Temperature was controlled and monitored using calibrated Si diodes.

3. Results

3.1. Phase transitions above room temperature

3.1.1. Dielectric studies. Figure 1(a) depicts the temperature variation of the real part (ε') of the dielectric constant for $x = 0.40$. A small peak in $\varepsilon'(T)$ occurs at 364 K. The dielectric constant above 364 K follows a Curie–Weiss law, $\varepsilon'(T) \sim C/(T - T_c)$, with a negative value of T_c ($=-130$ K) (see the lower inset to figure 1(a)). As shown earlier [1], a negative value of T_c is a signature of an AFE phase transition and hence the dielectric anomaly in figure 1(a) is due to an AFE phase transition. As can be seen from the upper inset to figure 1(a), the dielectric

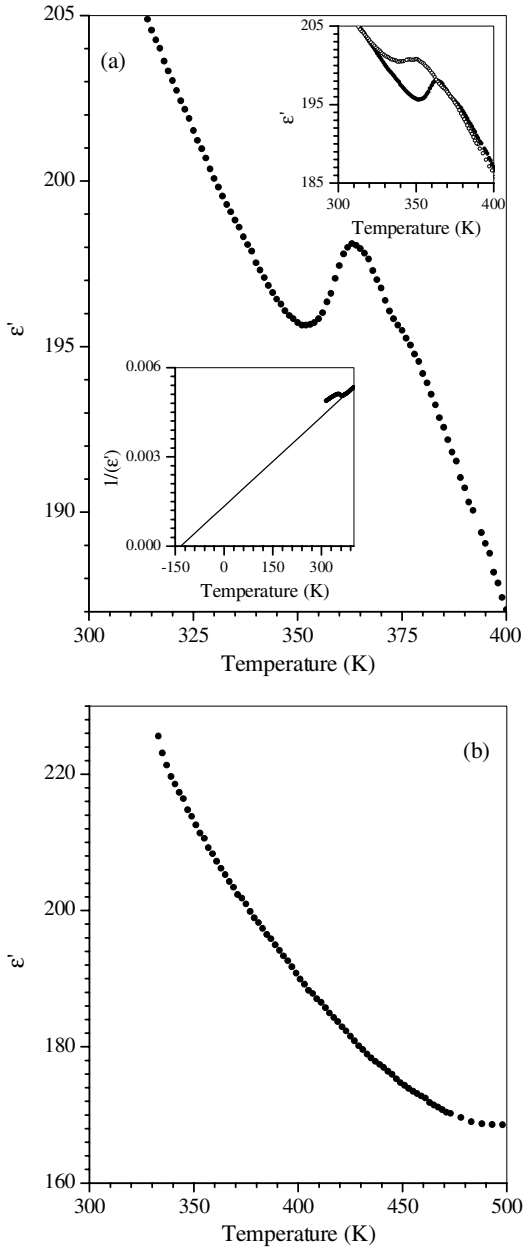

Figure 1. Temperature variation of the real (ε') part of the dielectric constant measured at 10 kHz for $Sr_{1-x}Ca_xTiO_3$ with (a) $x = 0.40$ and (b) $x = 0.43$. The lower inset in (a) shows the variation of dielectric stiffness (ε'^{-1}) with temperature for $x = 0.40$ and the upper inset depicts the temperature variation of ε' during heating and cooling of the sample.

constant peaks at 364 and 354 K during heating and cooling cycles respectively, exhibiting a thermal hysteresis of ∼10 K. This shows that the AFE phase transition is of first order. The AFE phase transition temperature of SCT is known [2] to increase at the rate of ≈11 K/mol% of $CaTiO_3$ in $SrTiO_3$. At this rate, one expects that, for $x = 0.43$, the AFE transition should occur around 400 K. No dielectric anomaly is, however, observed for this composition in the temperature range 325–500 K (see figure 1(b)). This, therefore, clearly indicates the absence of AFE phase for $x = 0.43$ in agreement with the structural studies of part I, where we showed the absence of AFE superlattice reflections for this composition at room temperature.

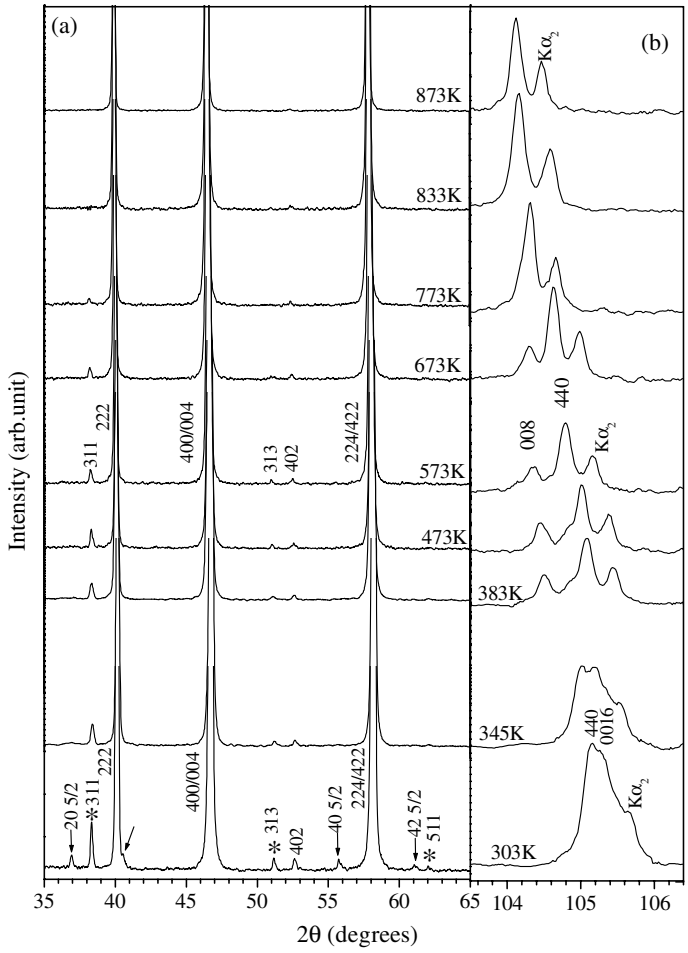

Figure 2. Evolution of the XRD pattern of $Sr_{0.60}Ca_{0.40}TiO_3$ (SCT40) with temperature in the 2θ range (a) 35°–65° and (b) 103.5°–106.5°. The arrows mark the antiferroelectric superlattice peaks which are not related to simple octahedral tilts while the asterisks mark the superlattice peaks due to octahedral tilts. The Miller indices in (a) are with respect to the doubled perovskite cell. As a result, the third index (l) of the antiferroelectric superlattice reflections has fractional numbers. The indices in (b) are with respect to the paraelectric ($Ibmm$) unit cell above 364 K and antiferroelectric ($Pbcm$) unit cell above this temperature.

3.1.2. X-ray diffraction studies

Phase transitions in SCT40. The powder XRD patterns given in figure 2 for $x = 0.40$ show that the AFE superlattice reflections, marked with arrows in the 303 K pattern, have disappeared at 383 K, i.e. above the AFE phase transition temperature of 364 K. Another remarkable feature accompanying the AFE transition is a significant change in the profile shapes of the main Bragg peaks such as 440 and 0016 reflections shown in figure 2(b). These two reflections of the AFE phase nearly overlap with each other at 303 K. Above the AFE transition temperature, the 0016 peak, which becomes 008 of the paraelectric (PE) phase, appears well separated from the 440 peak. We have assigned the space group $Ibmm$ to the PE phase on the basis of the considerations discussed in section 4.3 of part I. Thus, the 'nearly cubic'-like feature of the

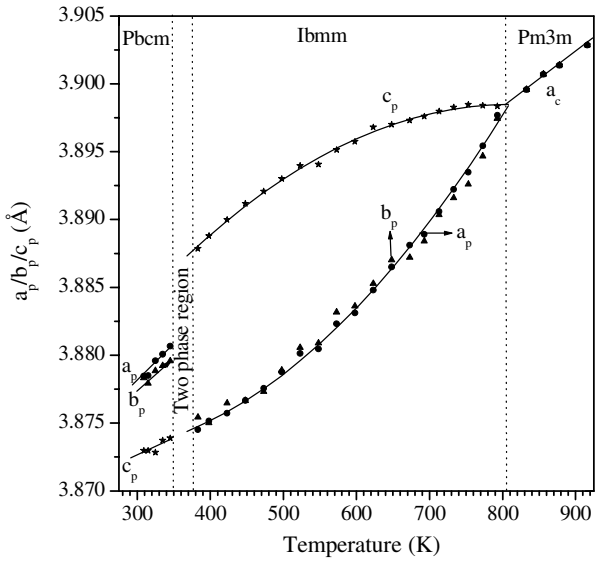

Figure 3. Evolution of the equivalent perovskite cell parameters (a_p, b_p and c_p) of $Sr_{0.60}Ca_{0.40}TiO_3$ (SCT40) above room temperature showing the presence of two transitions.

profiles at 303 K changes to pseudo-tetragonal-like in the PE phase. On heating the paraelectric phase, the superlattice peaks, characteristic of the anti-phase octahedral tilting (e.g. the 311 peak in figure 2) associated with the R ($q = \frac{1}{2}\ \frac{1}{2}\ \frac{1}{2}$) point instability, disappear above 800 K, as can be seen from the XRD pattern at 833 K in figure 2. The pseudo-tetragonal splitting of the 008 and 440 reflections has also disappeared at this temperature, indicating a transition to the cubic perovskite structure ($Pm3m$ space group) above 800 K.

The orthorhombic cell parameters of the AFE and PE phases at various temperatures were obtained by the Rietveld technique using $Pbcm$ and $Ibmm$ space groups, respectively. Figure 3 depicts the variation of elementary perovskite cell parameters (a_p, b_p and c_p) as a function of temperature. It is evident from this figure that at the AFE phase transition temperature both the parameters ($a_p \approx b_p$ and c_p) change discontinuously. The discontinuous change in the cell parameters provides additional confirmation about the first order nature of the AFE-PE phase transition in SCT. The difference in the a_p and b_p parameters of the $Ibmm$ phase was not resolvable.

Phase transitions in SCT43. Figures 4(a) and (b) depict the powder x-ray diffraction patterns of SCT43 in the 2θ range 35°–65° and 103.5°–106.5°, respectively, as a function of temperature. On heating, the intensity of the 'odd–odd–even' type (e.g. 310 near $2\theta = 36.5°$) superlattice reflections, resulting from the M ($q = \frac{1}{2}\ \frac{1}{2}\ 0$) point phonon instability, decreases and finally vanishes around 463 K. Above 463 K, only the 'odd–odd–odd' type superlattice reflections survive, which are characteristic of the R ($q = \frac{1}{2}\ \frac{1}{2}\ \frac{1}{2}$) point phonon instabilities.

Similar to the AFE transition for $x = 0.40$, the in-phase tilt transition for $x = 0.43$ is also accompanied by a drastic change in the shape of the profiles of the main Bragg peaks as shown in figure 4(b) for the 440 and the 008 reflections of the $Pbnm$ space group. The nearly overlapping 440 and 008 reflections at 300 K become well separated at $T \geqslant 463$ K. Further, the patterns at 463 and 573 K reveal coexistence of reflections characteristic of the room temperature and higher temperature phases. This suggests that the in-phase tilt transition is of first order type. The 008 and 440 reflections merge into one around 833 K when the structure becomes cubic ($Pm3m$).

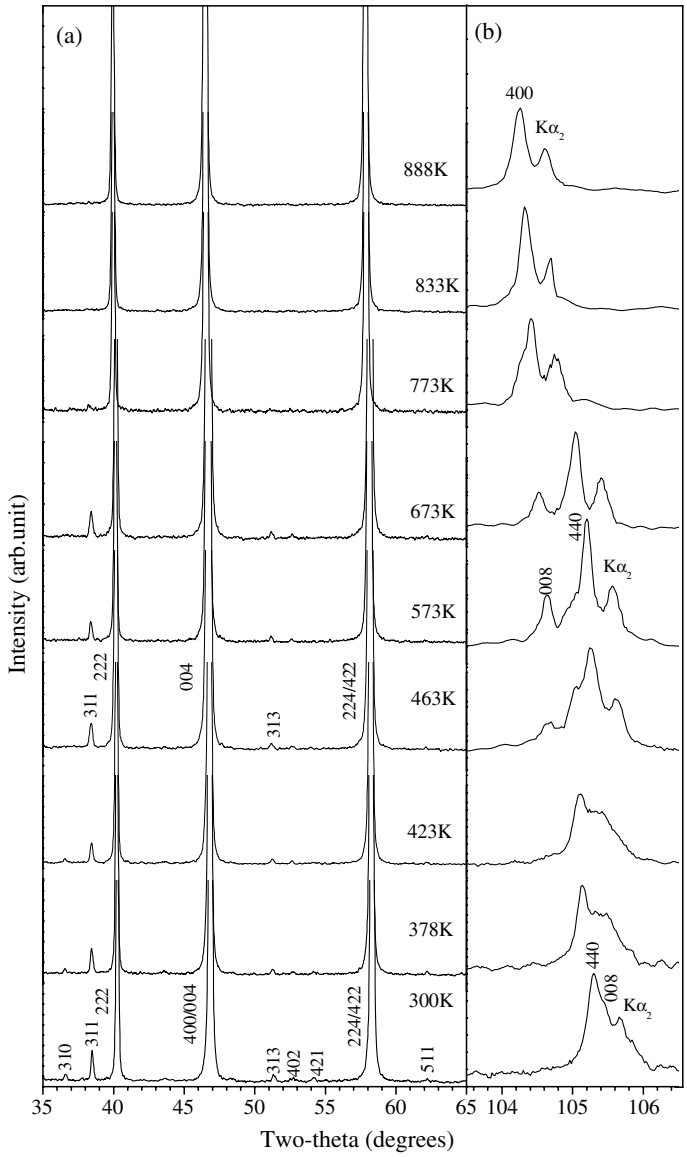

Figure 4. Evolution of the XRD pattern of $Sr_{0.57}Ca_{0.43}TiO_3$ (SCT43) with temperature in the 2θ range (a) 35°–65° and (b) 103.5°–106.5°. The Miller indices of the non-cubic phases are with respect to the doubled perovskite cell in (a) and orthorhombic ($Pbnm$) and tetragonal ($I4/mcm$) unit cell in (b).

The successive disappearance of the in-phase and anti-phase tilts is similar to that reported for $CaTiO_3$ for which a sequence of space group changes from $Pbnm$ to $I4mcm$ to $Pm3m$ has been reported in the literature [3, 4]. Accordingly, we carried out the Rietveld refinements of the structures of SCT43 using $Pbnm$, $I4/mcm$ and $Pm3m$ space groups in the temperature ranges 300 K $\leqslant T <$ 463 K, 463 K $< T <$ 835 K and $T >$ 835 K, respectively. Figure 5 shows the variation of the elementary perovskite cell parameters (a_p, b_p and c_p) with temperature. It is evident from this figure that all three lattice parameters change discontinuously at the $Pbnm$ to

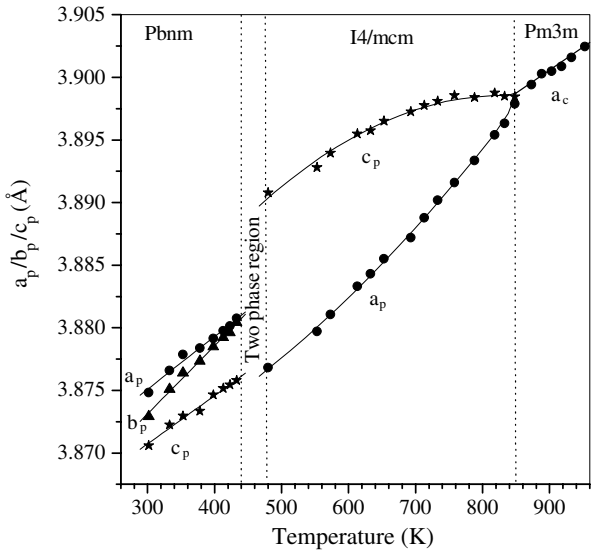

Figure 5. Evolution of the elementary perovskite cell parameters (a_p, b_p and c_p) of $Sr_{0.57}Ca_{0.43}TiO_3$ (SCT43) above room temperature showing the presence of two transitions.

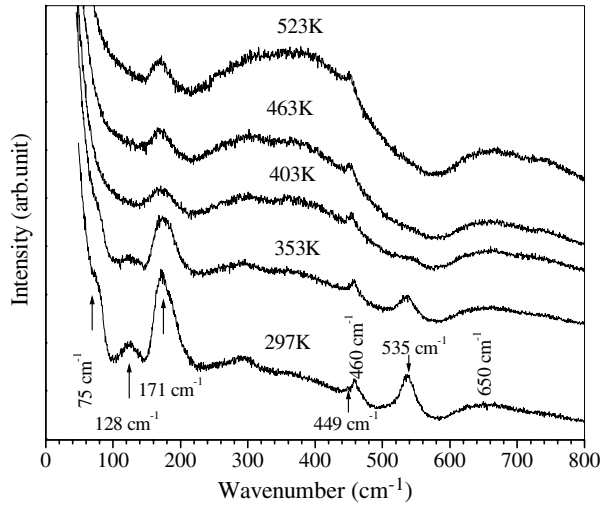

Figure 6. Evolution of the Raman spectra of $Sr_{0.60}Ca_{0.40}TiO_3$ (SCT40) as a function of temperature above room temperature.

$I4/mcm$ phase transition temperature, which lies somewhere between 440 and 480 K. The a_p and b_p parameters of the $Pbnm$ phase approach each other and nearly merge at the transition temperature, above which they undergo a discontinuous contraction. The c_p parameter, on the other hand, expands discontinuously at the same temperature. On further heating, both c_p and a_p parameters of the tetragonal phase approach each other until they merge at $T \approx 850$ K, at which the structure changes from tetragonal to cubic ($Pm3m$).

3.1.3. Raman scattering studies. The evolution of the Raman spectra of SCT40 with temperature is shown in figure 6. At room temperature (297 K), the Raman spectra of SCT40 contain first order Raman bands near the wave numbers 75, 128, 171, 449, 460 and 535 cm^{-1} besides second order Raman bands centred around 300 and 650 cm^{-1}. On heating, the bands near 75 and 128 cm^{-1} disappear in the PE phase as can be seen from the Raman spectra at $T \geqslant 403$ K. Further, there is a drastic decrease in the intensity of the bands at ∼171 and

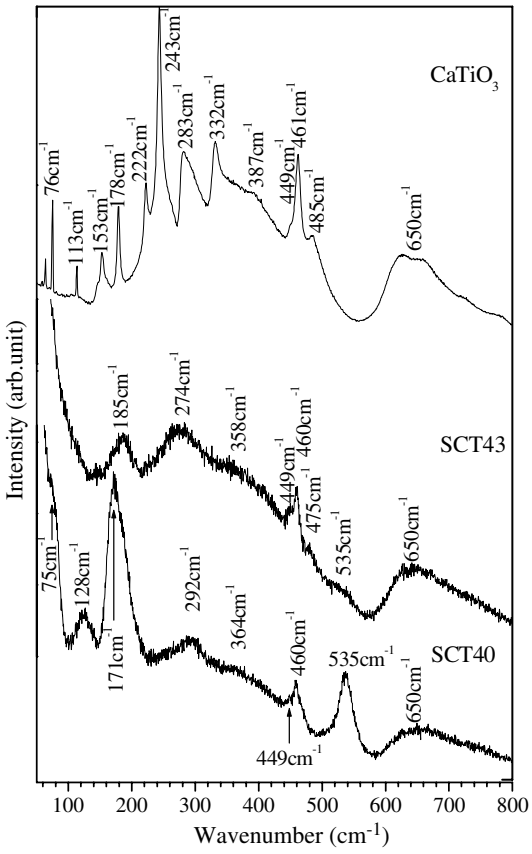

Figure 7. A comparison of the Raman spectra of $Sr_{0.57}Ca_{0.43}TiO_3$ (SCT43) with those of $Sr_{0.60}Ca_{0.40}TiO_3$ (SCT40) and $CaTiO_3$ (CT) at room temperature.

$\sim$535 cm^{-1} in the Raman spectra at $T \geqslant 403$ K. Both these features are similar to those observed in the evolution of the Raman spectra of SCT30 below room temperature across the PE to AFE phase transition temperature [5]. Thus, Raman scattering studies further confirm that SCT40 at room temperature is AFE, similar to the low temperature phase of SCT30.

Before discussing the high temperature phase transitions in SCT43, we first compare the room temperature Raman spectra of SCT43 with those of SCT40 and pure $CaTiO_3$ in figure 7. The Raman spectrum of SCT43 has some features similar to those found in $CaTiO_3$. The broad bands centred around 185, 274 and 358 cm^{-1} correspond to the cluster of Raman lines of $CaTiO_3$ around these frequencies. Disorder due to Sr^{2+} substitution has led to the broadening and banding of several of the first order Raman lines of $CaTiO_3$ in SCT43. The three sharp lines around 449, 460 and 475 cm^{-1} of SCT43 correspond to the modes at 449, 461 and 485 cm^{-1} of $CaTiO_3$. The first two of these three modes of SCT43 at 449 and 460 cm^{-1} are also similar to the 449 and 460 cm^{-1} lines of SCT40, but the other Raman line at 475 cm^{-1} in SCT43 is not present in SCT40. Also, the Raman lines at 75 and 128 cm^{-1} of SCT40 are absent in SCT43. Further, the room temperature Raman spectrum of SCT43 shows a weak broad band around 535 cm^{-1}, which is not present in pure $CaTiO_3$ but is a prominent line of SCT40. The presence of this mode in the *Pbnm* phase of SCT43 could be due to the proximity of this composition to the AFE–PE phase boundary ($x = 0.40$) at room temperature.

The Raman spectra of SCT43 do not show any drastic change as a function of temperature (see figure 8(a)) except for a sharp decrease in the wavenumber of the Raman line near

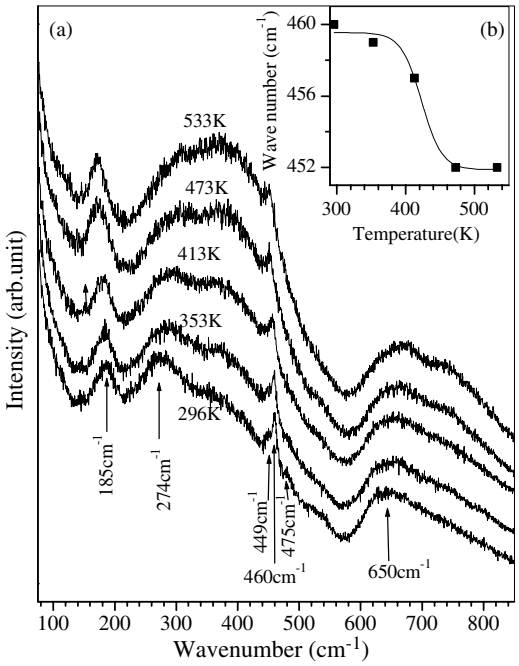

Figure 8. (a) Evolution of the Raman spectra of $Sr_{0.57}Ca_{0.43}TiO_3$ (SCT43) as a function of temperature. The temperature dependence of the frequency of one of the Raman lines is shown in inset (b).

460 cm^{-1} (see figure 8(b)) from 460 cm^{-1} at room temperature to 452 cm^{-1} at 473 K. Further, there is a strong modulation of the intensity of the second order Raman band near 380 cm^{-1} on raising the temperature from 296 to 473 K. The disappearance of the 310 superlattice reflection also occurs around the same temperature (∼473 K). Thus the discontinuous change in the frequency of the 460 cm^{-1} mode and the intensity modulation around 380 cm^{-1} seem to be linked with the vanishing of the in-phase tilt of the oxygen octahedra.

Due to experimental limitations of the Raman scattering set-up, it was not possible to record the Raman spectra above 533 K and hence the last transition to the cubic phases of $x = 0.40$ and 0.43 could not be monitored using Raman scattering data. However, the results presented in this section clearly show that the room temperature Raman spectra and their evolution above room temperature are entirely different for $x = 0.40$ and 0.43.

3.2. Phase transition studies below room temperature

3.2.1. SCT40. It is interesting to note from figure 1(a) for SCT40 that the dielectric constant, after peaking at the AFE phase transition temperature (∼364 K), starts rising again on lowering the temperature below ∼350 K. This points towards the possibility of a second dielectric anomaly at lower temperatures. On cooling below room temperature, Ranjan *et al* [6] have indeed reported that SCT40 exhibits a broad dielectric anomaly near 150 K. The phase below 150 K has been termed as the 'unknown' phase by Ranjan *et al* [6] since the origin of this transition is not clear. In order to see if this broad anomaly is linked with some structural change, we carried out low temperature x-ray diffraction measurements on SCT40 in the temperature range 300–12 K. We do not find any modification of the XRD patterns down to 12 K, at the level of the resolution of our diffractometer (see figure 9). However, the elementary perovskite cell parameters of SCT40, as obtained from Rietveld refinement of the structure using the *Pbcm* space group at various temperatures down to 12 K, do show saturation at

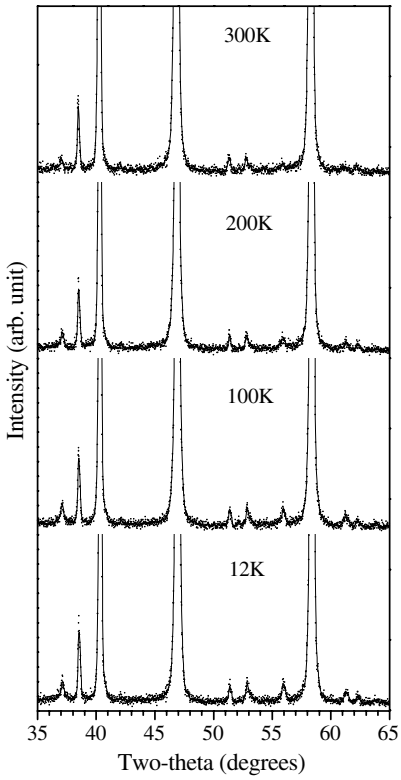

Figure 9. Evolution of the XRD pattern of $Sr_{0.60}Ca_{0.40}TiO_3$ (SCT40) with temperature in the 2θ range 35°–65° below room temperature.

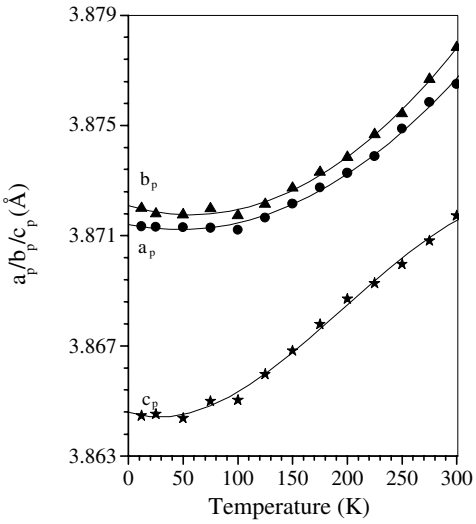

Figure 10. Evolution of the elementary perovskite cell parameters of $Sr_{0.60}Ca_{0.40}TiO_3$ (SCT40) below room temperature, showing their saturation at low temperatures.

low temperatures (see figure 10), which seems to be linked with the broad dielectric anomaly. Further support in evidence of this transition is found in the Raman spectra of SCT40 recorded at $T < 300$ K (see figure 11). It can be seen that the modes at ∼128 and ∼180 cm^{-1} split into two lines at lower temperatures. The temperature variation of the integrated intensity of the Raman band near 550 cm^{-1} (normalized with respect to the intensity of the mode at 460 cm^{-1}) reveals two slope changes around 360 and 150 K (see figure 12). The slope change near 360 K coincides with the AFE to PE phase transition temperature, while the second change of slope at 150 K matches very well with the peak temperature of the diffuse dielectric anomaly reported by Ranjan *et al* [6]. All these observations clearly confirm the existence of a low temperature transition in SCT40 occurring around 150 K.

3.2.2. SCT43. The real part of the dielectric constant of SCT43 continuously increases on lowering the temperature and shows a tendency for saturation at $T \leqslant 30$ K (see figure 13) similar to that reported for pure $CaTiO_3$ [7]. The only difference with respect to pure $CaTiO_3$ is in terms of higher dielectric constant values of SCT43 especially at low temperatures, which is due to Sr^{2+} substitution at the Ca^{2+} site. Although there is no anomaly in the temperature variation of the real part of the dielectric constant for $x = 0.43$, the imaginary part of the dielectric

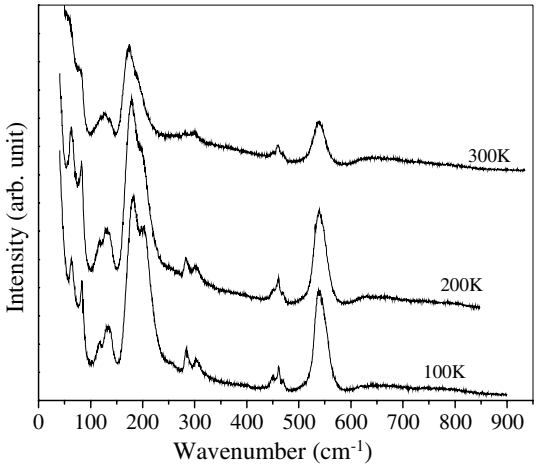

Figure 11. Evolution of the Raman spectra of $Sr_{0.60}Ca_{0.40}TiO_3$ (SCT40) as a function of temperature below room temperature.

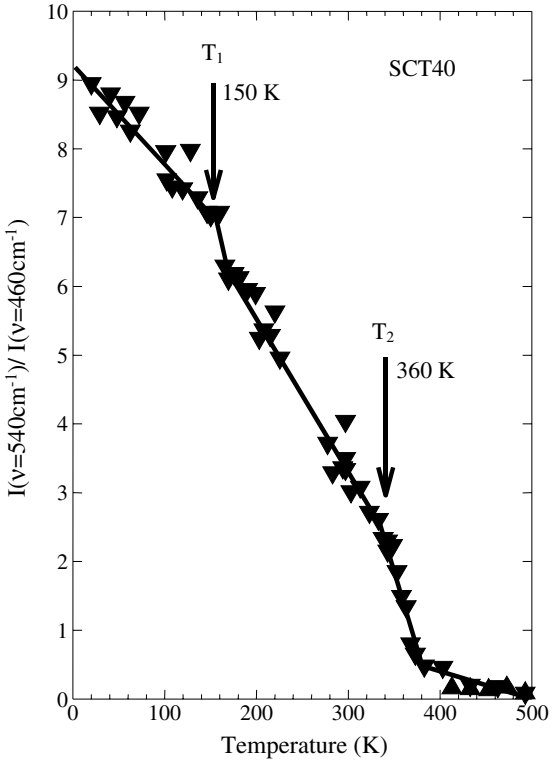

Figure 12. Temperature dependence of the integrated intensity of the Raman band ~550 cm^{-1}, normalized with the intensity of the Raman band at 460 cm^{-1}, for $Sr_{0.60}Ca_{0.40}TiO_3$. Arrows mark two transitions in SCT40.

constant does show a peak around 100 K, which indicates a phase transition. This low temperature phase transition is also confirmed by XRD and Raman measurements as explained below.

Figure 14 shows the temperature evolution of the XRD patterns of SCT43 in the temperature range 12–300 K. All the peaks at 300 K can be indexed with respect to the *Pbnm* space group. The XRD patterns at low temperatures do not show any perceptible change down to 12 K, expect for a weak intensity anomaly in the 440 and 008 (orthorhombic indices) pair of reflections. The intensities of these reflections become comparable at $T \leqslant 125$ K.

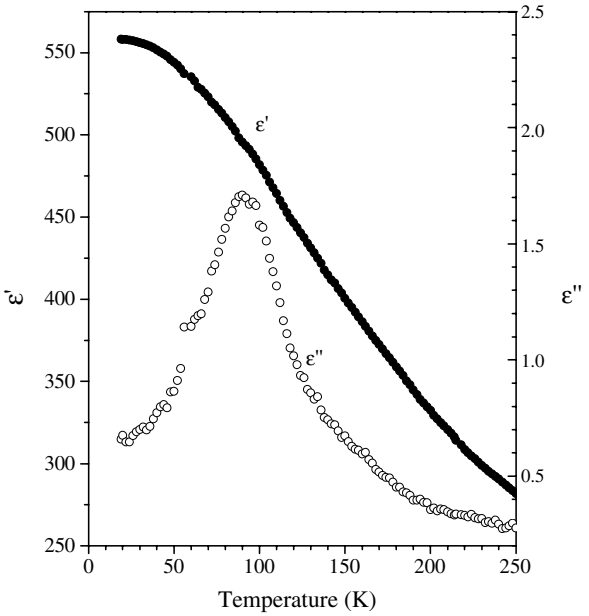

Figure 13. Temperature variation of the real (ε') and imaginary (ε'') parts of the dielectric constant of $Sr_{0.57}Ca_{0.43}TiO_3$ (SCT43) below room temperature.

However, this weak intensity anomaly is not convincing enough to be taken as evidence for a phase transition. It was found that the XRD data down to 12 K could be fitted to the $Pbnm$ space group by the Rietveld technique. However, the temperature variation of the elementary perovskite cell parameters, obtained after Rietveld refinement at each temperature, shows a distinct change of slope around 100 K (see figure 15), suggesting a phase transition near the same temperature where the peak in $\varepsilon''(T)$ occurs. The most convincing evidence for this low temperature phase transition comes from the Raman spectra of SCT43 at low temperatures. At $T \leqslant 98$ K, there is an increase in the intensity of the mode around 545 cm^{-1} (see figure 16). Also, a new Raman line at ~325 cm^{-1} becomes discernible. The appearance of a peak in the imaginary part of the dielectric constant, an anomaly in the unit cell parameters, and the modification of the Raman spectra around 100 K clearly suggest the occurrence of a new phase transition in SCT43 at low temperatures.

It is interesting to note that a similar low temperature transition to a monoclinic $P2_1/m$ has been proposed in $KMnF_3$ whose space group at room temperature is same as the $Pbnm$ space group of the room temperature phase of SCT43 [8]. The software ISOTROPY [9] predicts two monoclinic phases $P2_1/m$ and $P2_1/c$ based on the group–subgroup criterion. It is, however, not possible to confirm or refute the possibility of monoclinic distortion in the low temperature phase of SCT43 on the basis of the XRD data available with us. The monoclinic distortion, if any, is so small that only higher resolution synchrotron data on a highly homogeneous sample can capture it.

4. Conclusion

In this paper, we have shown that the nature of phase transitions as a function of temperature is markedly different for the two 'nearly cubic' compositions $x = 0.40$ and 0.43 of $Sr_{1-x}Ca_xTiO_3$. SCT40 undergoes an antiferroelectric transition around 364 K involving a change of space group from $Pbcm$ to $Ibmm$, followed by an antiferrodistortive phase transition from the anti-phase tilted $Ibmm$ structure to the untilted cubic ($Pm3m$) phase at ~800 K.

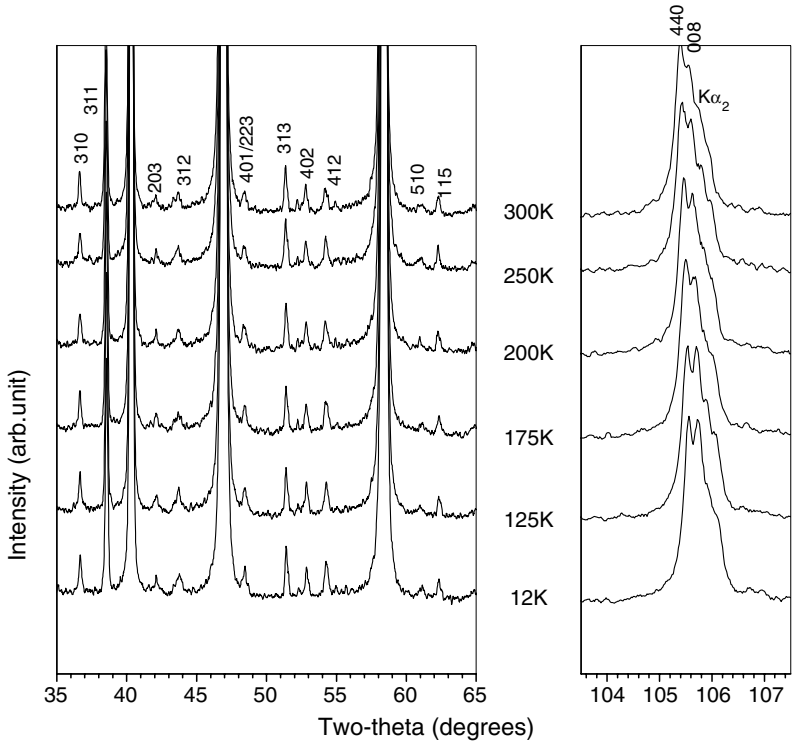

Figure 14. Evolution of the XRD pattern of $Sr_{0.57}Ca_{0.43}TiO_3$ (SCT43) with temperature in the 2θ range (a) 35°–65° and (b) 103.5°–107.3°. The Miller indices of the non-cubic phases are with respect to the doubled perovskite cell in (a) and the orthorhombic ($Pbnm$) and tetragonal ($I4/mcm$) unit cell in (b).

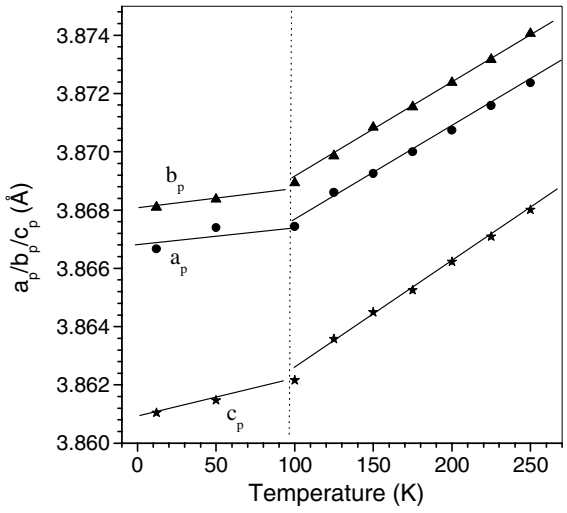

Figure 15. Evolution of the elementary perovskite cell parameters of $Sr_{0.57}Ca_{0.43}TiO_3$ (SCT43) below room temperature.

SCT43, on the other hand, exhibits two antiferrodistortive phase transitions linked with in-phase and anti-phase tilting of oxygen octahedra at 463 and 835 K, respectively. This transitions involve a change of space group from $Pbnm$ to $I4/mcm$ at 463 K and $I4/mcm$ to $Pm3m$ at

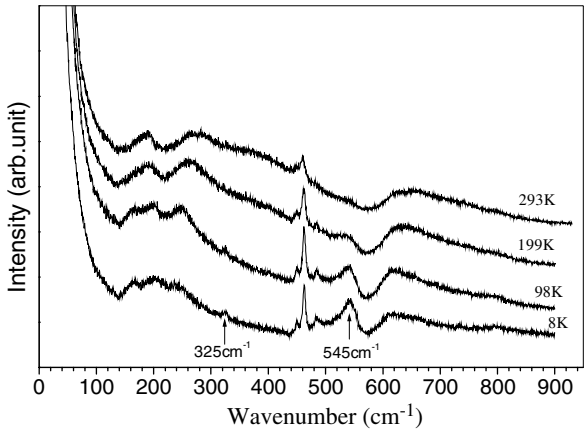

Figure 16. Evolution of the Raman spectra of $Sr_{0.57}Ca_{0.43}TiO_3$ (SCT43) as a function of temperature below room temperature.

835 K. Further, we have shown evidence for two different types of phase transitions below room temperature in SCT40 and SCT43. The nature and origin of these low temperature transitions is, however, not clear at this stage.

Acknowledgments

SKM is grateful to the Council of Scientific and Industrial Research (CSIR) of India for the award of a Senior Research Fellowship. RR gratefully acknowledges DST, Government of India, for financial support. DP acknowledges the UGC-DAE Consortium for Scientific Research for financial support.

References

[1] Ranjan R and Pandey D 2001 *J. Phys.: Condens. Matter* **13** 4239
[2] Ranjan R and Pandey D 2001 *J. Phys.: Condens. Matter* **13** 4251
[3] Redfern S A T 1996 *J. Phys.: Condens. Matter* **8** 8267
[4] Kennedy B J, Howard C J and Chakoumakos B C 1999 *J. Phys.: Condens. Matter* **11** 1479
[5] Mishra S K, Ranjan R, Pandey D, Ouillon R, Pinan-Lucarre J P, Ranson P and Pruzan Ph 2001 *Phys. Rev.* B **64** 092302
[6] Ranjan R, Pandey D and Lalla N P 2000 *Phys. Rev. Lett.* **84** 3726
[7] Kim I S, Itoh M and Nakamura T 1992 *J. Solid State Chem.* **101** 77
[8] Kapusta J and Daniel P 1999 *Phys. Rev.* B **59** 14235
[9] Stokes H T and Hatch D M 2005 ISOTROPY software and documentation is available over the internet at http://stokes.byu.edu/isotropy.html